

Sensor Fault Detection in Vehicle Lateral Control Systems via Switching Kalman Filtering

Tesheng Hsiao and Masayoshi Tomizuka

Department of Mechanical Engineering,

University of California at Berkeley, Berkeley, CA94720-1740

tshsiao@berkeley.edu tomizuka@me.berkeley.edu

Abstract – Vehicle lateral control for Automated Highway Systems (AHSs) is concerned with lane keeping and lane changing. It is of critical importance for safe highway operations; it must have fault tolerant capability in order to maintain stability in the event of malfunction of its components. In this paper, we investigate detection, isolation and accommodation of sensor faults. We propose a stochastic framework to which *switching Kalman filtering* and the *EM algorithm* are applied to detect faulty sensors and achieve good state estimation. With prior knowledge about the sensor failure modes, multiple sensors can be integrated into the framework, and the single failure assumption is no longer required. Simulations show that the sensor faults are detected immediately after their occurrences. Stability and performance are observed to be satisfactory in the event of sensor failures.

1. Introduction

The California PATH (Partner of Advanced Transit and Highways) Program has conducted an extensive study on Automated Highway Systems (AHSs) for reducing traffic congestion and enhancing safety. Driving tasks are carried out automatically by on-board sensors, actuators and computers without human intervention. The vehicle's lateral control system, one of the vital subsystems in AHS, acquires the lateral position from the lateral sensing system and generates steering command to keep the vehicle running along the road centerline. The lateral sensing system consists of magnetic markers embedded along the road centerline every 1.2 meter and two sets of magnetometers installed under the vehicle's front and rear bumpers [3][10]. Experiments have shown that the "look-ahead" scheme utilizing these two sets of magnetometers' outputs results in good control performance [3]. It has also been shown, however, that the performance of the scheme is sensitive to failures of the magnetometers [10]. In order to guarantee a safety operation, the lateral control system must have fault tolerant capability such that the system maintains stability and acceptable performance even when either set of magnetometers fails.

We have proposed an observer-based fault tolerant control scheme to detect, identify and accommodate magnetometers' failures in [5]. The scheme is canonical in

the sense that only two sets of magnetometers are required to accomplish fault detection and identification (FDI) and state estimation. It is, however, applicable only to two-output systems and is based on the *single failure assumption* which states that at most one sensor can fail at any time. There is no systematic way to integrate other on-board sensors such as gyros and accelerometers into the proposed observer-based structure and to relax the restrictive single failure assumption.

In this paper, we make use of *a priori* knowledge of the sensor failure modes to represent the fault signal as a *mixture of Gaussians model* [1][2]. A stochastic observer, switching Kalman filter or mixture Kalman filter [1][2][8], is designed to approximate the optimal state estimator in both normal and sensor failure cases. Failures will be detected and identified during the process of state estimation. The proposed stochastic observer structure can be extended to incorporate as many sensors as we want at the price of increasing computation load. Multiple sensor failures are allowed provided that the system is still observable with the outputs of the remaining healthy sensors.

This paper is organized as follows: Section 2 gives the bicycle model for vehicle lateral motion and the probability model imposed to the sensor failures. Design of switching Kalman filters is discussed in Section 3. The EM algorithm [9], which is used to compensate the unknown disturbance caused by the road curvature, is introduced in Section 4. Simulation results are presented in Section 5. Conclusions are given in Section 6.

2. Models and Problem Setting

2.1 Bicycle model

The bicycle model is widely used in the design of vehicle lateral controllers. Under the assumptions of a small steering angle and yaw angle, negligible roll and pitch motion, and linear tire model, the lateral motion can be expressed by a 4th order linear differential equation [4].

$$\dot{\mathbf{x}} = \mathbf{A}\mathbf{x} + \mathbf{B}_1\delta + \mathbf{B}_2d \quad (1)$$

$$\mathbf{y} = [y_1 \quad y_2 \quad y_3]^T = \mathbf{C}\mathbf{x} \quad (2)$$

The state \mathbf{x} consists of lateral position/velocity and yaw angle/rate. The output vector \mathbf{y} consists of the measurements from the two sets of magnetometers (y_1 and

y_2) and the gyro (y_3)¹. The disturbance d introduced by the road curvature is unknown. \mathbf{A} , \mathbf{B}_1 , \mathbf{B}_2 , and \mathbf{C} are known matrices shown below. The meaning of each symbol is listed in Table 1.

$$\mathbf{A} = \begin{bmatrix} 0 & 1 & 0 & 0 \\ 0 & -(\phi_1 + \phi_2) & (\phi_1 + \phi_2) & -\phi_1 l_1 + \phi_2 l_2 \\ 0 & \frac{v_x}{0} & 0 & \frac{v_x}{1} \\ 0 & -\frac{2(l_1 C_{af} - l_2 C_{ar})}{I_z v_x} & \frac{2(l_1 C_{af} - l_2 C_{ar})}{I_z} & -\frac{2(C_{af} l_1^2 + C_{ar} l_2^2)}{I_z v_x} \end{bmatrix}$$

$$\mathbf{B}_1 = \begin{bmatrix} 0 & \phi_1 & 0 & \frac{2C_{af} l_1}{I_z} \end{bmatrix}^T, \phi_1 = \frac{2C_{af}}{m}, \phi_2 = \frac{2C_{ar}}{m}$$

$$\mathbf{B}_2 = \begin{bmatrix} 0 & \frac{\phi_2 l_2 - \phi_1 l_1 - v_x^2}{v_x} & 0 & -\frac{2(C_{af} l_1^2 + C_{ar} l_2^2)}{I_z v_x} \end{bmatrix}^T$$

$$\mathbf{C} = \begin{bmatrix} 1 & 0 & d_1 & 0 \\ 1 & 0 & -d_2 & 0 \\ 0 & 0 & 0 & 1 \end{bmatrix}$$

Let \mathbf{C}_i denotes the i -th row of \mathbf{C} ; then $(\mathbf{A}, \mathbf{C}_1)$ and $(\mathbf{A}, \mathbf{C}_2)$ are observable whereas $(\mathbf{A}, \mathbf{C}_3)$ is not. In other words, full state estimation is still possible if the gyro and either set of the magnetometers have failed.

Table 1 nomenclature of the bicycle model

ε	yaw angle	δ	steering angle
m	mass	v_x	longitudinal speed
I_z	yaw moment of inertia		
d	disturbance caused by the road curvature		
l_1/l_2	distance between the front/rear wheel and the CG		
d_1/d_2	distance between the CG and the front/rear bumper		
C_{af}/C_{ar}	Cornering stiffness of the front/rear wheels		

The lateral sensing system may suffer from the following types of failures [10]:

(F1) Since the magnetometers are quite close to the ground, it is very likely that the magnetometers are hit by obstacles on the road and their signals can be lost. We model this situation as $y_i \sim N(0, \sigma_1^2)$, i.e. the corresponding output y_i is a Gaussian random process with zero mean and variance σ_1^2 .

(F2) The on-board lateral sensing system includes a preliminary fault detection mechanism. When faults are detected, the outputs of the corresponding magnetometers are set to its maximum values, which is 0.5. We model this situation as $y_i \sim N(0.5, \sigma_2^2)$.

(F3) The gyro could lose its information by accident. We model this situation as $y_3 \sim N(0, \sigma_3^2)$.

2.2 Probability Model

For convenience, we will derive the state estimation algorithm in discrete-time domain. Therefore the continuous-time model (1) and (2) are converted into the discrete-time counterparts (3) and (4). The output equation (4) is modified to include the effects of different types of sensor failures.

$$\mathbf{x}_{k+1} = \mathbf{A}_d \mathbf{x}_k + \mathbf{B}_{1d} \delta_k + \mathbf{B}_{2d} d_k \quad (3)$$

$$\mathbf{y}_k = \sum_{i=0}^M z_k^i \mathbf{y}_k^i = \sum_{i=0}^M z_k^i (\mathbf{C}_d^i \mathbf{x}_k + \mathbf{f}_k^i) \quad (4)$$

where \mathbf{y}_k^0 denotes the healthy sensor output and \mathbf{y}_k^i denotes the sensor's output under the i -th failure mode for $i > 0$. $z_k^i \in \{0, 1\}$ is unknown and selects *exactly one* of the \mathbf{y}_k^i 's at each step k . \mathbf{f}_k^i 's are Gaussian processes.

$$\mathbf{f}_k^i \sim N(\boldsymbol{\mu}^i, \mathbf{V}^i), i=0,1,\dots,M, \forall k \quad (5)$$

where $\boldsymbol{\mu}^0 = \mathbf{0}$ and $\mathbf{V}^0 = \sigma_0^2 \mathbf{I}$ denote the mean and variance of the measurement noise under no sensor failures. \mathbf{C}_d^i , $\boldsymbol{\mu}^i$, and \mathbf{V}^i , $i=0,\dots,M$, are assumed to be known and represent different failure modes. For example, \mathbf{y}_k^1 represents the sensor output when the front set of magnetometers undergoes failure (F1) and other sensors work properly, then

$$\mathbf{C}_d^1 = [\mathbf{0}; \mathbf{C}_{d,2}; \mathbf{C}_{d,3}], \boldsymbol{\mu}^1 = \mathbf{0}, \text{ and } \mathbf{V}^1 = \text{diag}(\sigma_1^2, \sigma_0^2, \sigma_0^2)$$

z_k^i is regarded as a *multinomial* random variable for each k . Since z_k^i depends on z_{k-1}^i (the sensor broken at step $k-1$ is more likely to remain broken at step k and thereafter.), we assume z_k^i is a *Markov-chain* random process, i.e.

$$p(z_k^i = 1) = \pi^i \text{ and } \sum_{i=0}^M \pi^i = 1 \quad (6)$$

$$p(z_k^j = 1 | z_{k-1}^i = 1) = \pi^{i,j}, i, j = 0,1,\dots,M, \forall k \quad (7)$$

π^i is the *prior probability* of the occurrence of the i -th failure mode. $\pi^{i,j}$ is the *conditional probability* of the occurrence of the j -th type of failure at step k , given the occurrence of the i -th type of failure at step $k-1$. π^i and $\pi^{i,j}$ are assumed to be known. They can be derived from prior knowledge about the quality of the sensors.

We also model the initial state \mathbf{x}_0 and disturbance d_k to be Gaussian random variables, i.e.

$$\mathbf{x}_0 \sim N(\boldsymbol{\mu}_{\mathbf{x}_0}, \mathbf{X}_0) \text{ and } d_k \sim N(\mu_k^d, \sigma_d^2) \quad (8)$$

where $\boldsymbol{\mu}_{\mathbf{x}_0}$ and \mathbf{X}_0 are assumed to be known. Note that in reality d_k is deterministic and the probabilistic description of d_k seems artificial. However σ_d can be viewed as a design parameter for the designer to adjust the Kalman filter gain. μ_k^d depends on the road curvature which is unknown and varies with time. As in the standard setting of Kalman filtering, we assume \mathbf{f}_k^i , d_k , and \mathbf{x}_0 are independent.

Remarks:

(a) \mathbf{y}_k^i is Gaussian for each i whereas \mathbf{y}_k is not. The density function of \mathbf{y}_k is a convex combination of Gaussian density functions. In other words, \mathbf{y}_k is expressed as a *mixture of Gaussians model* [1][2][7]. Efficient algorithms to estimate the state of the mixture of Gaussians model will be

¹ Due to the DC drift problem, applying the gyro measurement is more elaborate than that presented in this paper. The implementation issue is beyond the scope this paper. It is included in the output vector to demonstrate that the single failure assumption is not necessary.

discussed in the next section.

(b) Under the probabilistic setting, the FDI problem is equivalent to evaluate the posterior probabilities:

$$p(z_k^i | \mathbf{y}_0, \dots, \mathbf{y}_k) = \tau_k^i \quad i=0,1,\dots,M. \quad (9)$$

Let $\tau_k^j = \max\{\tau_k^0, \dots, \tau_k^M\}$. If $j=0$, then there is no sensor failure at step k ; otherwise the j -th failure mode has taken place.

2.3 Problem Statement

Given model descriptions (3)~(8) and a stabilizing controller, we will derive a real-time algorithm to detect, identify and accommodate sensor failures such that stability and acceptable performance are achieved when parts of sensors have failed. No single failure assumption is made in this approach. To accommodate sensor failures, the algorithm must be capable of estimating the state reasonably well despite the occurrence of failures. The controller generates the steering command based on the estimated state.

Figure 1 is the block diagram of the proposed closed loop system, where SKF denotes switching Kalman filter which will be illustrated in the next section.

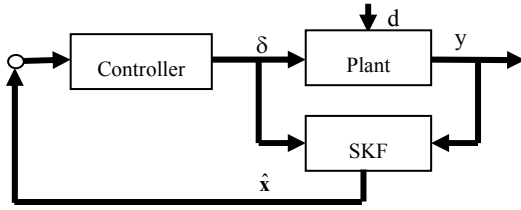


Figure 1 Block diagram of the proposed closed loop system

The standard Kalman filtering algorithm is applicable only to Gaussian processes. For non-Gaussian cases, it is mathematically intractable to compute exactly the “optimal” estimated state (in the sense of minimum variance). Moreover, μ_k^d is unknown and time-varying. A special algorithm tailored to the present application will be derived in the next two sections.

3. Switching Kalman Filter

In this section, we assume that μ_k^d is known and focus on the state estimation problem under mixture of Gaussian processes. Several methods have been proposed in the literatures, e.g. *Monte Carlo filtering* [1] or “*splitting and collapsing*” method [7][8]. The latter is more efficient and often provides satisfactory results. It is reviewed below. First of all we introduce the following notations:

$$\begin{aligned} \mathbf{y}_{[s,t]} &= \{\mathbf{y}_s, \mathbf{y}_{s+1}, \dots, \mathbf{y}_t\} \text{ for any } s < t. \\ \hat{\mathbf{x}}_{s|t}^{i,j} &= E[\mathbf{x}_s | \mathbf{y}_{[0,t]}, z_{s-1}^i = 1, z_s^j = 1] \\ \hat{\mathbf{x}}_{s|t}^i &= E[\mathbf{x}_s | \mathbf{y}_{[0,t]}, z_s^i = 1] \\ \mathbf{P}_{s|t}^{i,j} &= Var[\mathbf{x}_s | \mathbf{y}_{[0,t]}, z_{s-1}^i = 1, z_s^j = 1] \end{aligned}$$

$$\mathbf{P}_{s|t}^i = Var[\mathbf{x}_s | \mathbf{y}_{[0,t]}, z_s^i = 1]$$

$$L_k^{i,j} = p(\mathbf{y}_k | \mathbf{y}_{[0,k-1]}, z_{k-1}^i = i, z_k^j = j)$$

$$\tau_{k,k+1}^{i,j} = p(z_k^i = 1, z_{k+1}^j = 1 | \mathbf{y}_{[0,k+1]})$$

If the values of z^i 's are specified, the optimal state estimation problem becomes a standard Kalman filtering problem. Given the estimated state at step k , the “splitting process” applies the standard Kalman filtering algorithm repeatedly to compute $M+1$ state estimates at step $k+1$, each of which corresponds to $z_{k+1}^i=1$ for $i=0,\dots,M$ respectively. The splitting process continues and generates $(M+1)^2$ estimated states at step $k+2$. The number of estimated states blows up exponentially. See Figure 2 for $M=1$.

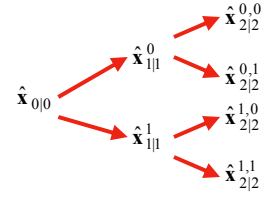


Figure 2 Splitting process for $M=1$

To make the problem tractable, there must be a “collapsing” mechanism to reduce the number of estimated states. The GPB(2) algorithm (Generalized Pseudo Bayesian algorithm of order 2, [8]) maintains $(M+1)^2$ estimated states $\hat{\mathbf{x}}_{k|k}^{i,j}$ at each step k by collapsing $M+1$ estimated states $\hat{\mathbf{x}}_{k|k}^{i,j}$, $i=0,1,\dots,M$ into one estimate, $\hat{\mathbf{x}}_{k|k}^j$. See Figure 3 for $M=1$.

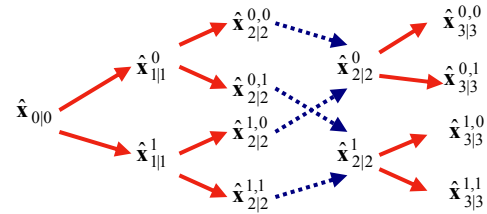


Figure 3 Splitting and collapsing processes for $M=1$. Real line: splitting. Dotted line: collapsing.

The “splitting and collapsing” algorithm is recursive. Given $(\hat{\mathbf{x}}_{k|k}^i, \mathbf{P}_{k|k}^i, \tau_{k|k}^i)$ at step k , compute $(\hat{\mathbf{x}}_{k+1|k+1}^i, \mathbf{P}_{k+1|k+1}^i, \tau_{k+1|k+1}^i)$ at the next step. See Algorithm 1 below or references [7] and [8] for more details.

Algorithm 1:

Splitting:

$$\begin{aligned} \hat{\mathbf{x}}_{k+1|k}^i &= \mathbf{A}_d \hat{\mathbf{x}}_{k|k}^i + \mathbf{B}_{1d} \delta_k + \mathbf{B}_{2d} \boldsymbol{\mu}_k^d \\ \mathbf{P}_{k+1|k}^i &= \mathbf{A} \mathbf{P}_{k|k}^i \mathbf{A}^T + \sigma_d^2 \mathbf{B}_{2d} \mathbf{B}_{2d}^T \\ \boldsymbol{\eta}_{k+1}^{i,j} &= \mathbf{y}_{k+1} - \mathbf{C}_d^j \hat{\mathbf{x}}_{k+1|k}^i - \boldsymbol{\mu}^j \\ \mathbf{S}_{k+1|k}^{i,j} &= \mathbf{C}_d^j \mathbf{P}_{k+1|k}^i (\mathbf{C}_d^j)^T + \mathbf{V}^j \end{aligned}$$

$$\begin{aligned}\hat{\mathbf{x}}_{k+1|k+1}^{i,j} &= \hat{\mathbf{x}}_{k+1|k}^i + \mathbf{P}_{k+1|k}^i (\mathbf{C}_d^j)^T (\mathbf{S}_{k+1|k}^{i,j})^{-1} \boldsymbol{\eta}_{k+1}^{i,j} \\ \mathbf{P}_{k+1|k+1}^{i,j} &= \mathbf{P}_{k+1|k}^i - \mathbf{P}_{k+1|k}^i (\mathbf{C}_d^j)^T (\mathbf{S}_{k+1|k}^{i,j})^{-1} \mathbf{C}_d^j \mathbf{P}_{k+1|k}^i\end{aligned}$$

Collapsing

$$\begin{aligned}L_{k+1}^{i,j} &= (2\pi)^{-\frac{M}{2}} \det(\mathbf{S}_{k+1|k}^{i,j})^{-\frac{M}{2}} \exp\left\{-\frac{1}{2}(\boldsymbol{\eta}_{k+1}^{i,j})^T (\mathbf{S}_{k+1|k}^{i,j})^{-1} \boldsymbol{\eta}_{k+1}^{i,j}\right\} \\ \tau_{k,k+1}^{i,j} &= \frac{1}{Z} L_{k+1}^{i,j} \pi^{i,j} \tau_k^i \quad \text{where } Z = \sum_{i,j=0}^M L_{k+1}^{i,j} \pi^{i,j} \tau_k^i \\ \tau_{k+1}^j &= \sum_{i=0}^M \tau_{k,k+1}^{i,j}, \quad \hat{\mathbf{x}}_{k+1|k+1}^j = \frac{1}{\tau_{k+1}^j} \sum_{i=0}^M \tau_{k,k+1}^{i,j} \hat{\mathbf{x}}_{k+1|k+1}^{i,j} \\ \mathbf{P}_{k+1|k+1}^j &= \frac{1}{\tau_{k+1}^j} \sum_{i=0}^M \left[\mathbf{P}_{k+1|k+1}^{i,j} + \tilde{\mathbf{x}}_{k+1}^{i,j} (\tilde{\mathbf{x}}_{k+1}^{i,j})^T \right], \quad \tilde{\mathbf{x}}_{k+1}^j = \hat{\mathbf{x}}_{k+1|k+1}^j - \hat{\mathbf{x}}_{k+1|k+1}^i \\ \hat{\mathbf{x}}_{k+1|k+1}^i &= \sum_{j=0}^M \tau_{k+1}^j \hat{\mathbf{x}}_{k+1|k+1}^{i,j}\end{aligned}$$

Remark:

We can derive algorithms which compute $(M+1)^3$ estimates $\hat{\mathbf{x}}_{k|k}^{i,j,m} = E[\mathbf{x}_k | z_k^i = 1, z_{k-1}^j = 1, z_{k-2}^m = 1]$ at each step k and then collapse them into $(M+1)^2$ estimates. It results in a better approximation since more Gaussian processes are involved; however the computation load increases exponentially.

4. EM Algorithm

4.1 EM-algorithm in General

The EM algorithm is a generic iterative algorithm to estimate unknown parameters when some of the random variables are unobserved (called *latent* variables). It consists of two steps: Expectation step (E-step) and Maximization step (M-step). The idea behind the EM-algorithm is to separate a complex problem into two simple but coupled problems. Solve one problem at a time assuming that the answer of the other problem is known and continue the process iteratively.

For example, let \mathbf{X} and \mathbf{Y} be random variables with joint probability $p(\mathbf{X}, \mathbf{Y} | \theta)$, where \mathbf{Y} is observed, \mathbf{X} is latent and θ is the unknown parameter to be estimated. The maximum likelihood estimation is

$$\hat{\theta}_{ML} = \arg \max_{\theta} \{L(\theta) = \log p(x, y | \theta)\} \quad (10)$$

Solving the optimization problem (10) directly is often a daunting task because both \mathbf{X} and θ are unknown. The EM-algorithm provides a two-step iterative solution:

$$\text{E - step : } \hat{L}(\theta^{t-1}) = E_{p(x|y)}[L(\theta^{t-1})]$$

$$\text{M - step : } \theta^t = \arg \max_{\theta} \hat{L}(\theta^{t-1})$$

where θ^t is the estimate of θ at the t -th iteration. E-step assumes θ 's value from the previous iteration and computes the "best" estimate of \mathbf{X} by averaging out the likelihood function with respect to the conditional probability $p(\mathbf{X} | \mathbf{Y})$. M-step maximizes the (averaged) likelihood function from E-step to update the current estimate of θ . The procedure keeps going until θ converges. It can be shown that the EM-algorithm does converge to the local maximum of the *complete log likelihood function*, $\log p(\mathbf{X}, \mathbf{Y} | \theta)$ [9].

4.2 Estimating μ_k^d by EM algorithm

In the lateral control problem, the state \mathbf{x} is latent and μ_k^d is the unknown parameter. We apply the EM algorithm to estimate both \mathbf{x} and μ_k^d in this subsection. First, we write down the complete log likelihood function at step k .

$$\begin{aligned}L &= \log p(\mathbf{x}_{[0:k+1]}, \mathbf{y}_{[0:k]}, z_{[0:k]}) \\ &= \sum_{t=0}^k \log p(\mathbf{x}_{t+1} | \mathbf{x}_t) + \sum_{t=0}^k \log p(\mathbf{y}_t | \mathbf{x}_t, z_t) \\ &\quad + \sum_{t=1}^k \log p(z_t | z_{t-1}) + \log p(z_0) + \log p(\mathbf{x}_0)\end{aligned}$$

Since the disturbance \mathbf{d}_t is piecewise constant, we assume that μ_t^d is constant within a "N-duration window" around each step k , i.e. $\mu_t^d = \mu^d$ for $t \in [k-N+1, k]$. Note that only the conditional density functions $p(\mathbf{x}_{t+1} | \mathbf{x}_t)$, $t \in [k-N+1, k]$, are related to μ^d . Other terms of L disappear after we take derivatives of L with respect to μ^d . Therefore we redefine the log likelihood function L which includes only N terms related to μ^d .

$$L(\mu^d) = \sum_{t=k-N+1}^k \log p(\mathbf{x}_{t+1} | \mathbf{x}_t)$$

Note that $\mathbf{x}_{t+1} | \mathbf{x}_t \sim N(\mathbf{A}_d \mathbf{x}_t + \mathbf{B}_{1d} \delta_t + \mathbf{B}_{2d} \mu^d, \sigma_d^2 \mathbf{B}_{2d} \mathbf{B}_{2d}^T)$, where $\mathbf{B}_{2d} \mathbf{B}_{2d}^T$ is singular with rank 1. Let

$$\sigma_d^2 \mathbf{B}_{2d} \mathbf{B}_{2d}^T = \mathbf{U}^T \begin{bmatrix} \beta^2 & \mathbf{0} \\ \mathbf{0} & \mathbf{0} \end{bmatrix} \mathbf{U}, \quad \mathbf{U}^T \mathbf{U} = \mathbf{U} \mathbf{U}^T = \mathbf{I}$$

and $\mathbf{U} \mathbf{B}_{2d} = [\beta / \sigma_d \quad \mathbf{0}]^T$. Let $\mathbf{w}_t = \mathbf{U} \mathbf{x}_t$; \mathbf{U}_i and w_t^i denote the i -th row of \mathbf{U} and \mathbf{w}_t respectively. Then

$$\begin{aligned}p(\mathbf{x}_{t+1} | \mathbf{x}_t) &= p(\mathbf{w}_{t+1} | \mathbf{w}_t) \det \mathbf{U} \\ &= p(w_{t+1}^1 | \mathbf{w}_t) \prod_{i=2}^n \delta(w_{t+1}^i)\end{aligned}$$

where $w_{t+1}^1 | \mathbf{w}_t \sim N(\mathbf{U}_1 (\mathbf{A}_d \mathbf{x}_t + \mathbf{B}_{1d} \delta_t + \mathbf{B}_{2d} \mu^d), \beta^2)$. We modify the log likelihood function L again to exclude terms unrelated to μ^d .

$$L(\mu^d) = \sum_{t=k-N+1}^k \log p(w_{t+1}^1 | \mathbf{w}_t) = C - \frac{1}{2\beta^2} \sum_{t=k-N+1}^k (q_t - \frac{\beta}{\sigma_d} \mu^d)^2$$

where C is a constant and $q_t = \mathbf{U}_1 (\mathbf{x}_{t+1} - \mathbf{A}_d \mathbf{x}_t - \mathbf{B}_{1d} \delta_t)$

Next we derive E-step and M-step with respect to L :

E-step:

$$\begin{aligned}\hat{L} &= E[L | \mathbf{y}_{[0:k]}] \\ &= C - \frac{1}{2\beta^2} \sum_{t=k-N+1}^k \left(E[q_t^2 | \mathbf{y}_{[0:k]}] - 2 \frac{\beta}{\sigma_d} \mu^d E[q_t | \mathbf{y}_{[0:k]}] + \left(\frac{\beta}{\sigma_d} \mu^d \right)^2 \right)\end{aligned}$$

M-step:

$$\text{Let } \frac{\partial \hat{L}}{\partial \mu^d} = \frac{-1}{2\beta^2} \sum_{t=k-N+1}^k \left(\frac{-2\beta}{\sigma_d} \hat{q}_{t|k} + 2 \left(\frac{\beta}{\sigma_d} \right)^2 \mu^d \right) = 0 \quad (11)$$

where $\hat{q}_{t|k} = E[q_t | \mathbf{y}_{[0:k]}] = \mathbf{U}_1 (\hat{\mathbf{x}}_{t+1|k} - \mathbf{A}_d \hat{\mathbf{x}}_{t|k} - \mathbf{B}_{1d} \delta_t)$

$$\text{Then } \hat{\mu}^d = \frac{1}{N} \frac{\sigma_d}{\beta} \sum_{t=k-N+1}^k \hat{q}_{t|k} \quad (12)$$

Note that Eq. (12) requires a smoothing process at each step k to compute $\hat{\mathbf{x}}_{t|k}$ for $t \in [k-N+1, k]$. *Switching Kalman smoothing* is feasible but time-consuming. The smoothing algorithm includes implementation of Algorithm 1 in both forward and backward directions for each step and we found that it cannot be applied to our real-time control systems. Therefore we modify Eq. (11) by replacing the “N-duration window” with an exponential decay window.

Let $\sum_{t=0}^k \gamma^{k-t} \left(-\hat{q}_{t|k} + \frac{\beta}{\sigma_d} \mu_k^d \right) = 0$, where $0 < \gamma < 1$. Then $\hat{\mu}_k^d = \frac{1}{\Gamma_k} \frac{\sigma_d}{\beta} \sum_{t=0}^k \gamma^{k-t} \hat{q}_{t|k}$, where $\Gamma_k = \sum_{t=0}^k \gamma^{k-t}$ (13)

Expanding the summation in Eq. (13):

$$\begin{aligned} \sum_{t=0}^k \gamma^{k-t} \hat{q}_{t|k} &= \mathbf{U}_1 \sum_{t=0}^k \gamma^{k-t} (\hat{\mathbf{x}}_{t+1|k} - \mathbf{A}_d \hat{\mathbf{x}}_{t|k} - \mathbf{B}_{1d} \delta_t) \\ &= \mathbf{U}_1 (\hat{\mathbf{x}}_{k+1|k} - \mathbf{B}_{1d} \Delta_k - \gamma^{k+1} \hat{\mathbf{x}}_{0|k}) + \hat{s}_{k|k} \end{aligned}$$

where $\hat{s}_{k|k} = \mathbf{U}_1 (\gamma \mathbf{I} - \mathbf{A}_d) \sum_{t=0}^k \gamma^{k-t} \hat{\mathbf{x}}_{t|k}$, and $\Delta_k = \sum_{t=0}^k \gamma^{k-t} \delta_t$

For large k 's, $\gamma^{k+1} \hat{\mathbf{x}}_{0|k}$ is negligible. Then we have

$$\hat{\mu}_k^d = \frac{1}{\Gamma} \frac{\sigma_d}{\beta} \left[\mathbf{U}_1 (\hat{\mathbf{x}}_{k+1|k} - \mathbf{B}_{1d} \Delta_k) + \hat{s}_{k|k} \right] \quad (14)$$

Note that $\hat{s}_{k|k}$ is the conditional mean of

$s_k = \mathbf{U}_1 (\gamma \mathbf{I} - \mathbf{A}_d) \sum_{t=0}^k \gamma^{k-t} \mathbf{x}_t$ given $\mathbf{y}_{[0, \dots, k]}$. It can be obtained by applying the switching Kalman filtering algorithm to the augmented system (15) and (16) below.

$$\begin{aligned} \begin{bmatrix} \mathbf{x}_{k+1} \\ s_{k+1} \end{bmatrix} &= \begin{bmatrix} \mathbf{A}_d & \mathbf{0} \\ \mathbf{U}_1 (\gamma \mathbf{I} - \mathbf{A}_d) \mathbf{A}_d & \gamma \end{bmatrix} \begin{bmatrix} \mathbf{x}_k \\ s_k \end{bmatrix} + \begin{bmatrix} \mathbf{B}_{1d} \\ \mathbf{U}_1 (\gamma \mathbf{I} - \mathbf{A}_d) \mathbf{B}_{1d} \end{bmatrix} \delta_k \\ &+ \begin{bmatrix} \mathbf{B}_{2d} \\ \mathbf{U}_1 (\gamma \mathbf{I} - \mathbf{A}_d) \mathbf{B}_{2d} \end{bmatrix} d_k \end{aligned} \quad (15)$$

$$\mathbf{y}_k = \sum_{i=0}^M z_k^i \left(\begin{bmatrix} \mathbf{C}_d^i & \mathbf{0} \end{bmatrix} \begin{bmatrix} \mathbf{x}_k \\ s_k \end{bmatrix} + \mathbf{f}_k^i \right) \quad (16)$$

When Algorithm 1 is applied to (15) and (16), μ_k^d in Algorithm 1 is replaced by $\hat{\mu}_{k-1}^d$. Then substitute $\hat{s}_{k|k}$ into (14) to update the current estimate of μ^d . In this way, we can estimate both the state and the mean of the unknown disturbance in a real-time manner.

5. Simulation

In the following simulations, we set the longitudinal speed v_x to be 25 m/sec \approx 56 mph. The road curvature ρ is set to be 1/1000 (1/m). Hence the disturbance d_k is $v_x/\rho = 0.025$ [4]. Note that these settings are in accordance with the highway traffic in U.S. We set up 6 failure modes which are listed in Table 2.

The following parameters are selected: $\sigma_0 = 0.0075$, $\sigma_1 = \sigma_3 = 10\sigma_0$, $\sigma_2 = 0.1\sigma_0$ and $\sigma_d = 10^{-4}$. The prior probabilities π^{ij} 's are shown in Table 3. And $\pi^i = \pi^{0,i}$ (see eq. (6)); $\boldsymbol{\mu}_{x0} = \mathbf{0}$, $\mathbf{X}_0 = \mathbf{0}$ and $\gamma = 0.99$.

The selection of these parameters is based on the prior

knowledge of the sensors. For example, the value of σ_0 is chosen such that 99% of the measurement noise is within the range (-0.02 0.02). We set $\pi^{3,0} = 0.003$, $\pi^{3,3} = 0.995$ and $\pi^{3,4} = 0.002$ because the sensing system in failure mode 3 (the rear set of magnetometers suffers from failure F1) at step k is much more likely to stay at mode 3 at step $k+1$. It's also possible for it to jump to mode 0 (the magnetometer works again) or to mode 4 (the rear set of magnetometers suffers from failure F2).

Table 2 Failure modes

Mode			
0	Normal mode	3	y_2 is under failure F1
1	y_1 is under failure F1	4	y_2 is under failure F2
2	y_1 is under failure F2	5	y_3 is under failure F3
6	y_1 AND y_3 are under failures F2 and F3, respectively		

Table 3 the prior probabilities π^{ij}

π^{ij}	j=0	j=1	j=2	j=3	j=4	j=5	j=6
i=0	0.998	5e-4	3e-4	5e-4	4e-4	2e-4	1e-4
i=1	0.003	0.995	0.002	0	0	0	0
i=2	0.003	0.001	0.992	0	0	0	0.004
i=3	0.003	0	0	0.995	0.002	0	0
i=4	0.003	0	0	0.001	0.996	0	0
i=5	0.003	0	0	0	0	0.993	0.004
i=6	0	0.001	0.003	0	0	0.003	0.993

Case 1: In this case, failure mode 2 takes place at $7 \leq t \leq 12$ while failure mode 4 takes place at $14 \leq t \leq 24$. We can see from

Figure 4 that the corresponding τ^i 's becomes maximal among all posterior probabilities. The SKF performs state and disturbance estimation well under different failure modes and in the presence of disturbance. The disturbance affects the calculation of the posterior probabilities (part (g)). But the transient response caused by the disturbance dies out quickly once its effect has been compensated by the estimated disturbance.

Case 2²: In this case, we simulate the situation of concurrent sensor failures. y_1 undergoes failure F2 at $3 \leq t \leq 13$ while y_3 undergoes failure F3 at $7 \leq t \leq 17$. At $t \in [7, 13]$, y_1 and y_3 fail simultaneously, which is failure mode 6. We can see from Figure 5 that these faults are successfully detected and identified. The state estimation remains good under these failures.

² Control by the rear set of magnetometers only has been reported difficult in experiments [6] in the presence of model uncertainties, which is not reflected in the simulations. Current research efforts are directed to design robust observers to overcome this problem.

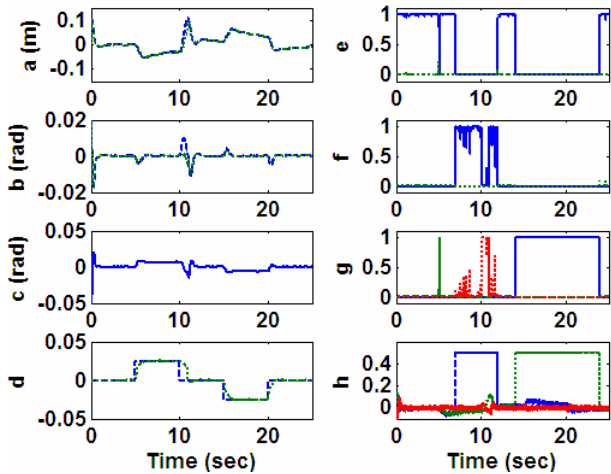


Figure 4 (a) dashed line (--): lateral position of the vehicle's C.G.; dotted line(:): estimated lateral position. (b) dashed line (--): the vehicle's yaw angle; dotted line (:): estimated yaw angle. (c) steering angle (d) dashed line (--): disturbance; dotted line (:): estimated disturbance (e) real line: τ^0 ; dotted line (:): τ^1 . (f) real line: τ^2 ; dotted line τ^3 . (g) real line: τ^4 ; dashed line: τ^5 ; dotted line: τ^6 . (h) dashed line (--): y_1 ; dotted line(:): y_2 ; solid line (-): y_3 .

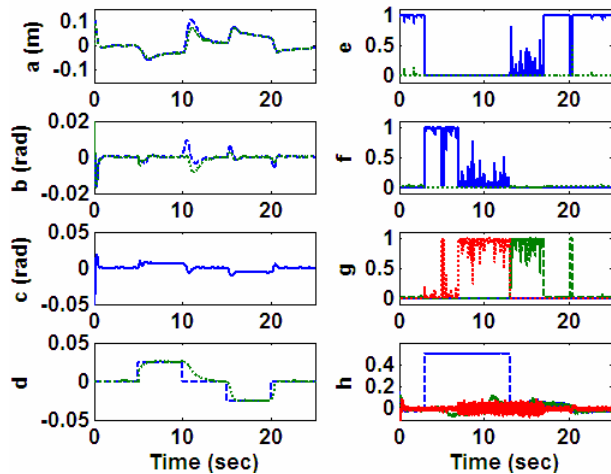


Figure 5 (a) dashed line (--): lateral position of the vehicle's C.G.; dotted line(:): estimated lateral position. (b) dashed line (--): the vehicle's yaw angle; dotted line (:): estimated yaw angle. (c) steering angle (d) dashed line (--): disturbance; dotted line (:): estimated disturbance (e) real line: τ^0 ; dotted line (:): τ^1 . (f) real line: τ^2 ; dotted line τ^3 . (g) real line: τ^4 ; dashed line: τ^5 ; dotted line: τ^6 . (h) dashed line (--): y_1 ; dotted line(:): y_2 ; solid line (-): y_3 .

6. Conclusion

In this paper, we cast the sensor FDI problem in a stochastic framework. Multiple sensor cases can be integrated into this framework in a systematic way provided we know a priori their failure modes. The single failure assumption is no longer required. To estimate the vehicle's state and compute the posterior probabilities for

FDI purpose under the proposed stochastic settings, we applied switching Kalman filtering and the EM algorithm. Simulations demonstrated that state and disturbance can be estimated reasonably well under either normal or sensor failure modes. The normal mode controller was able to stabilize the system and achieve acceptable performance by feeding back the estimated state instead of the sensor measurements. Experiments will be conducted to verify the proposed algorithm.

References

- [1] Chen, R. and Liu, J. S., *Mixture Kalman Filters*, Journal of the Royal Statistical Society (B), Vol. 62, 2000, pp493~508
- [2] Chen, R., Wang, X., and Liu, J. S., *Adaptive Joint Detection and Decoding in Flat-Fading Channels via Mixture Kalman Filtering*, IEEE Trans. on Information Theory, Vol. 46, No. 6, 2000, pp2079~2094
- [3] Guldner, J. Tan, H. and Patwardhan, S., *Study of Design Directions for Lateral Vehicle Control*, Proc. of the CDC 1997, pp4732~4737
- [4] Hingwe, P. S., *Robustness and Performance Issues in the Lateral Control of Vehicles in Automated Highway Systems*, Ph. D. Dissertation, UC Berkeley, 1997
- [5] Hsiao, T. and Tomizuka, M., *Observer-based Sensor Fault Detection and Identification with Application to Vehicle Lateral Control*, Proc. of the American Control Conference, 2004. pp810~815
- [6] Huang, J., and Tomizuka, M., *H_∞ controller for vehicle lateral control under fault in front or rear sensors*, Proc. of the American Control Conference, 2001, Vol. 2, pp690~695
- [7] Kim, C-J., *Dynamic Linear Models with Markov-Switching*, J. of Econometrics, 60, 1-22, 1994.
- [8] Murphy, K., *Learning Switching Kalman Filter Models*, Compaq Cambridge Research Lab Tech Report 98-10, 1998.
- [9] Neal, R. and Hinton, G., *A View of the EM Algorithm that Justifies Incremental, Sparse, and Other Variants*, Learning in Graphical Models, MIT Press, 1999, pp355~368
- [10] Suryanarayanan, S., *Fault Tolerant Control and its Application to Lane-keeping Control of Automated Vehicles*, Ph. D. Dissertation, UC Berkeley, 2002.